Dielectric and Thermodynamic Signatures of Low Temperature Glassy Dynamics in the Hybrid Perovskites $CH_3NH_3PbI_3$ and $HC(NH_2)_2PbI_3$

Douglas H. Fabini,[†,‡] Tom Hogan,[¶,‡] Hayden A. Evans,[†,§]
Constantinos C. Stoumpos,[∥] Mercouri G. Kanatzidis,[∥] and
Ram Seshadri[*,†,‡,§]

†*Materials Research Laboratory,*
University of California, Santa Barbara, California 93106, USA
‡*Materials Department, University of California, Santa Barbara, California 93106, USA*
¶*Department of Physics, Boston College, Chestnut Hill, Massachusetts 02467, USA*
§*Department of Chemistry and Biochemistry,*
University of California, Santa Barbara, California 93106, USA
∥*Department of Chemistry and Argonne-Northwestern Solar Energy Research (ANSER) Center, Northwestern University, Evanston, Illinois 60208, USA*

E-mail: seshadri@mrl.ucsb.edu

Abstract

Hybrid main group halide perovskites hold great technological promise in optoelectronic applications and present rich and complex evolution of structure and dynamics. Here we present low temperature dielectric measurements and calorimetry of $A\mathrm{PbI_3}$ [A = $\mathrm{CH_3NH_3^+}$, $\mathrm{HC(NH_2)_2^+}$] that suggest glassy behavior on cooling. In both compounds, the dielectric loss displays frequency-dependent peaks below 100 K characteristic of a glassy slowing of relaxation dynamics, with $\mathrm{HC(NH_2)_2PbI_3}$ exhibiting greater glass fragility. Consistent with quenched disorder, the low temperature heat capacity of both perovskites deviates substantially from the $\sim T^3$ acoustic phonon contribution predicted by the Debye model. We suggest that static disorder of the A-site molecular cation, potentially coupled to local distortions of the Pb–I sublattice, is responsible for these phenomena. The distinct low temperature dynamics observed in these two perovskites suggest qualitative differences in the interaction between the molecular cation and the surrounding inorganic framework, with potential implications for defect screening and device performance at ambient temperatures.

Graphical TOC Entry

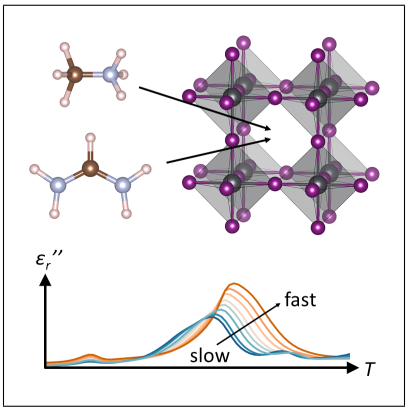

Hybrid organic–inorganic main group halide perovskites of the form AMX_3 [$A = CH_3NH_3^+$, $HC(NH_2)_2^+$; $M = Sn^{2+}$, Pb^{2+}; $X = Cl^-$, Br^-, I^-] have attracted intense research interest for their performance in photovoltaic (PV) and other optoelectronic devices, coupled with ease of preparation, and abundance of their constituent elements. In particular, $CH_3NH_3PbI_3$ (methylammonium lead iodide) has been the subject of numerous recent investigations since the first report of its application in a PV device in 2009.[1] Recently, high performance PV devices incorporating $HC(NH_2)_2PbI_3$ (formamidinium lead iodide) have been reported.[2] For both compositions, many reports have focused on characterizing devices and understanding photophysical and electronic processes, while far fewer efforts have sought to develop a detailed description of crystal structure and disorder.

Due to the importance of local electric fields and defect screening for carrier separation and extraction in devices, much recent work has focused on the local dielectric environment in related lone pair-bearing main group metal halides[3,4] and the relationship between long-range polarization and performance of field-effect transistors and PV devices employing $CH_3NH_3PbI_3$.[5,6] In addition to its importance in phase transitions in hybrid perovskites,[7–11] the *A*-site dipolar cation is an important determinant of dielectric properties.[12,13] Accordingly, much attention has been paid to the dynamics of the disordered molecular cations in $CH_3NH_3PbI_3$. Early ^2H nuclear magnetic resonance (NMR) investigations of N-deuterated samples indicate both rapid reorientation of the C–N axis with respect to the inorganic cage (hereafter, "tumbling") and rotation about the C–N axis (hereafter, "twisting") in the cubic and tetragonal phases, while only twisting remains in the low temperature orthorhombic phase.[14] Temperature studies of ^1H NMR spin-lattice relaxation times indicate the presence of cation twisting (activation energy 60 meV per molecule) in the orthorhombic phase and suggest rotational tunneling at temperatures below $\sim$70 K (first excited torsional state 23 meV above the ground state).[15] Based on calorimetry and infrared vibrational spectroscopy, three models of order–disorder transitions of the organic cation have been proposed, all of which imply a fully ordered organic

cation in the orthorhombic phase.[16] Dielectric measurements indicate tumbling of the organic cation in the cubic and tetragonal phases and a Curie-Weiss-like temperature dependence of the real permittivity, consistent with a thermally inhibited net polarization of the molecular dipoles in the presence of an applied field.[12] Group theoretical analysis of quasi-elastic neutron scattering experiments suggests the presence of a four-fold rotation (tumbling, $\sim$5 ps at ambient temperature) and a three-fold rotation (twisting, $\sim$1 ps at ambient temperature) in the cubic and tetragonal phases, but only the three-fold rotation in the orthorhombic phase (slowing substantially to $\sim$4 ns at 70 K).[17] Weller et al. refined crystallographic structure models from neutron powder diffraction that indicate isotropic disorder of the organic cation in the cubic and tetragonal phases.[11] In the orthorhombic phase, they find that the molecular point group symmetry is compatible with the crystal site symmetry and all atoms can be localized. In their model, the organic cations are ordered antiferroelectrically in the [010] direction, with alternating C–N dipole orientations from cell to cell. Despite the nominal full ordering of the hydrogen atoms, they find large anisotropic atomic displacement parameters (ADPs) that are consistent with substantial librations of the organic cation even at 100 K.[11] Lee et al. perform ab initio computational investigations of the orthorhombic phase which confirm the stability of the *trans* conformation of the organic cation and indicate hydrogen bonding between the amine-group hydrogens and the neighboring iodides of the inorganic cage.[18] Starting from the nominal structure of Weller et al. and fixing all other structure parameters, they find energy barriers (per molecule) of $\sim$70 meV, $\sim$190 meV, and $\sim$100 meV for three-fold rotation of the methyl group, amine group, and full molecule, respectively, implying that none of these modes are appreciably thermally populated in the orthorhombic phase.[18]

Far fewer reports of the structure and properties of $HC(NH_2)_2PbI_3$ exist to date. This compound exhibits polymorphism between a black perovskite phase and a yellow phase of 1-D chains at ambient temperatures, as well as further phase evolution on cooling.[10] We shall focus the remainder of our discussion on the perovskite phases. Trigonal structures

for the ambient and intermediate temperature phases have been reported on the basis of laboratory single crystal X-ray diffraction.[10] The structure of the ambient temperature phase has recently been clarified via neutron powder diffraction, which suggests the cubic *Pm*$\bar{3}$*m* perovskite aristotype and, correspondingly, a highly disordered molecular cation.[19] The structure of the low temperature phase below 140 K (transition temperature from differential scanning calorimetry, Supporting Information Figure S2) has not been fully resolved.

An overview of the crystal structure of the low temperature phase of $CH_3NH_3PbI_3$ and the high temperature phase of both compositions is given in Figure 1. In light of the conflicting evidence from various experimental and theoretical treatments of the degree of ordering of the organic cation in the orthorhombic phase of $CH_3NH_3PbI_3$, here we employ dielectric spectroscopy and calorimetry to study the disorder of the polar molecular ion, and we extend our analysis to the closely-related and relatively underexplored $HC(NH_2)_2PbI_3$. We find in both compounds, frequency-dependent dielectric loss peaks below 100 K characteristic of glassy slowing of relaxation dynamics. In $HC(NH_2)_2PbI_3$, the evidence points to greater glass fragility, perhaps due to the distinct shapes and dipole moments of the molecular cations. The low temperature heat capacity of both perovskites deviates substantially from the $C \sim T^3$ acoustic phonon contribution predicted by the Debye model. Some static disorder of the *A*-site molecular cation, potentially coupled to local distortions of the Pb–I sublattice, is suggested to play a role in these observed phenomena.

The complex permittivity across the full temperature range is presented in the Supporting Information (Figure S1) and confirms the reported behavior of the $CH_3NH_3^+$ cation at the tetragonal–orthorhombic phase transition.[12] At higher temperatures, the intrinsic permittivity is obscured by ionic conductivity[5,6,13,20] as well as interfacial and microstructural effects.[21–23] The low temperature complex permittivity is presented in Figure 2. Broad, frequency-dependent dielectric loss peaks are evident in both compositions, arising from the resonance of the probe with a dielectric relaxation process. Characteristic of glassy

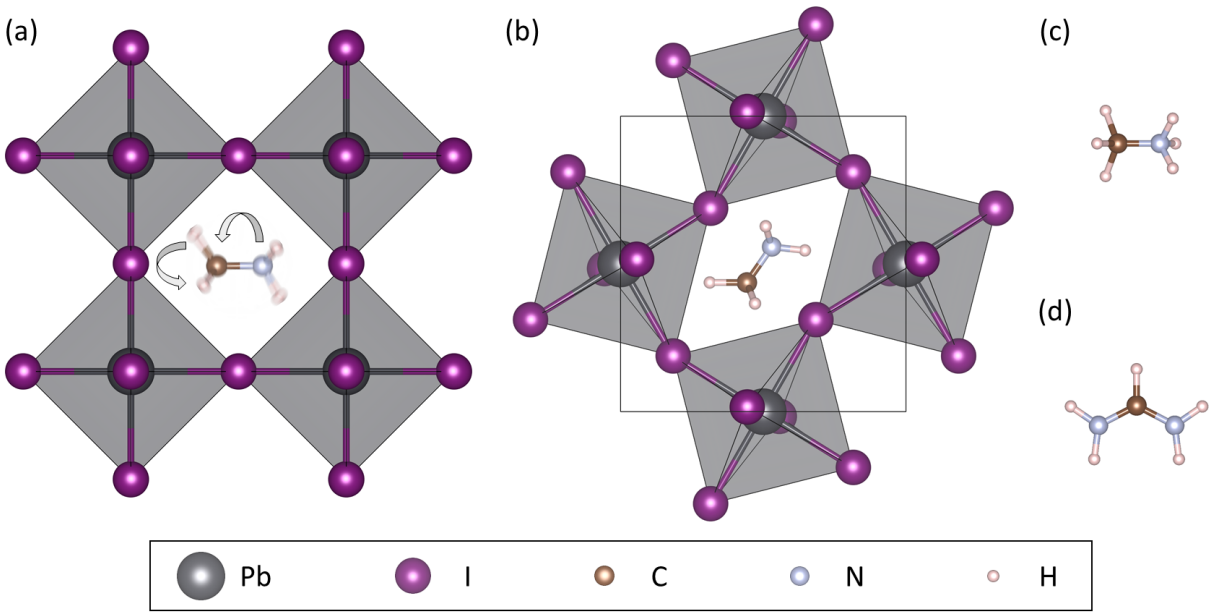

Figure 1: (a) High temperature cubic perovskite ($Pm\bar{3}m$) structure of $CH_3NH_3PbI_3$ (a = 6.31728(27) Å at 352 K)[11] and $HC(NH_2)_2PbI_3$ (a = 6.3620(8) Å at 300 K)[19] with highly disordered A-site cation. (b) Low temperature orthorhombic ($Pnma$) structure of $CH_3NH_3PbI_3$ at 100 K. Refined ADPs for the atoms of the organic cation remain large and anisotropic at this temperature.[11] Low temperature structures ($<$ 150 K) have not yet been reported for $HC(NH_2)_2PbI_3$. (c) Methylammonium ion, $[CH_3NH_3]^+$. (d) Formamidinium ion, $[HC(NH_2)_2]^+$.

behavior, the dynamics slow by many orders of magnitude as the sample is cooled towards the glass transition.[24–27] Importantly, the real part of the permittivity is minimally reduced as the relaxation is frozen out ($< 1\%$ for $CH_3NH_3PbI_3$, $< 7\%$ for $HC(NH_2)_2PbI_3$), suggesting that the relevant process does not involve significant reorientation of the C–N dipole axis. Though a wider spectral range is necessary to identify the functional form of the relaxation process and to model its temperature dependence,[25] we can readily conclude that at sufficiently low temperatures, both compositions exhibit a degree of static structural disorder. The feature seen in $HC(NH_2)_2PbI_3$ around 65 K is suppressed to varying degrees from sample to sample and may be due to extrinsic effects associated with impurities or sample preparation. Here, we focus our analysis on the most pronounced loss peaks (50 K to 80 K for $CH_3NH_3PbI_3$ and 40 K to 50 K for $HC(NH_2)_2PbI_3$). In addition to these frequency-disperse loss peaks, the frequency-independent feature at $\sim$13 K in the permittivity of $HC(NH_2)_2PbI_3$ suggests a structural phase transition that has not been reported.

The temperature-dependence of the relaxation dynamics is given in Figure 3. The glassy slowing is much more abrupt with temperature for $HC(NH_2)_2PbI_3$, suggesting that this compound exhibits more fragile glass dynamics,[25] an assertion which is corroborated by our calorimetry (*vide infra*). So-called "strong" glass-formers like SiO_2 exhibit substantial local structural similarity between the glass and the melt, while "fragile" glass-formers like toluene can take on a wide range of distinct configurations upon quenching and are often characterized by non-directional Coulomb or Van der Waals interactions.[25] The distinct dynamics observed in these two perovskites suggests that differences in molecular cation size, shape, and dipole moment give rise to qualitative differences in the mechanism of amorphization and the structure of the resulting statically disordered phases.

The heat capacities of both compositions are presented in Figure 4. As expected for soft crystals, the heat capacities rise rapidly with temperature and begin to level off as all phonon modes become appreciably populated.[28] The known $HC(NH_2)_2PbI_3$ first-order

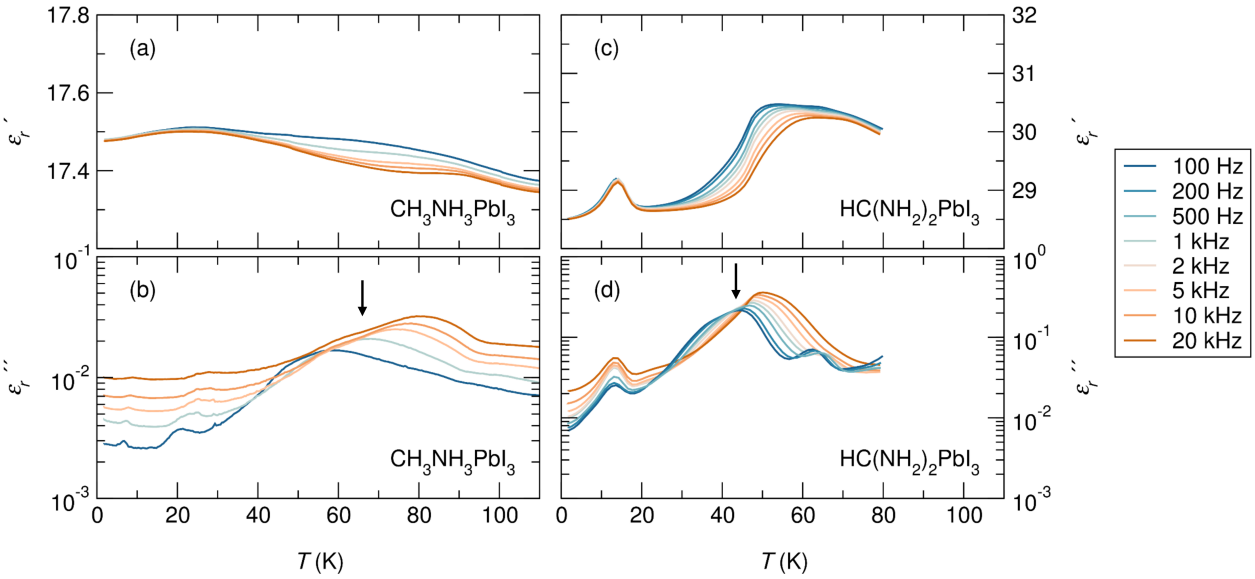

Figure 2: Low temperature detail of the real (ϵ_r') and imaginary (ϵ_r'') parts of the relative permittivity of polycrystalline (a,b) $CH_3NH_3PbI_3$ and (c,d) $HC(NH_2)_2PbI_3$ extracted from capacitance–loss measurements. Frequency-dependent dielectric loss peaks (↓) indicating substantial slowing of relaxation dynamics are observed in both samples. Additionally, a divergence in permittivity at 13 K for $HC(NH_2)_2PbI_3$ indicates a previously unreported structural phase transition.

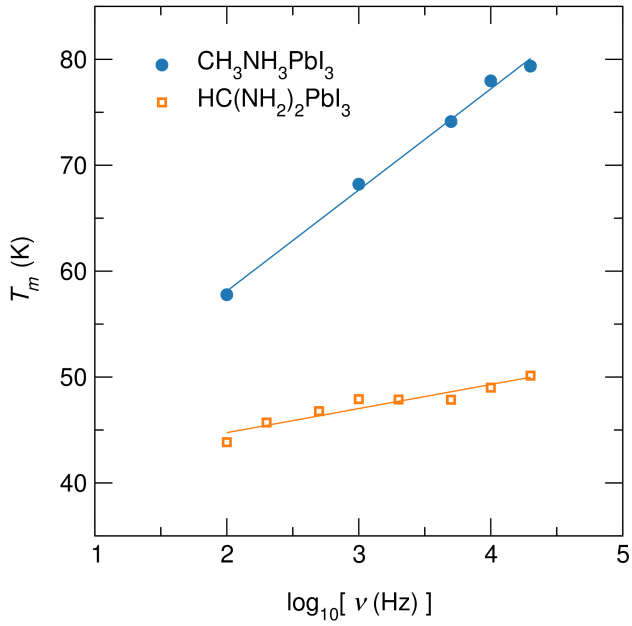

Figure 3: Temperature, T_m, of the low temperature dielectric loss peak versus probe frequency, ν. The stronger temperature dependence for $HC(NH_2)_2PbI_3$ suggests that this composition exhibits more fragile glass dynamics than $CH_3NH_3PbI_3$.

phase transition at ∼140 K (Supporting Information, Figure S2) is poorly captured with our logarithmic temperature sampling. At 150 K, the heat capacities of both compositions are well below the high temperature limit of 36*R* (gas constant $R = 8.314$ J mol^{-1} K^{-1}) predicted by Dulong and Petit for this crystal with a 12 atom formula unit.[28] Indeed, previously reported calorimetry of $CH_3NH_3PbI_3$ up to 360 K gives a constant heat capacity of ∼180 J mol^{-1} K^{-1} in the cubic phase. We postulate that this corresponds to saturation of 21 or 22 of the 36 vibrational modes possible in this crystal: the 15 translational modes of the inorganic atoms and molecular center of mass, the 3 rotational modes of the full molecule, and 3 or 4 unidentified moderately soft intramolecular modes such as hydrogen wagging or independent methyl and amine group rotations about the C–N axis. A similar plateau of heat capacity up to 300 K at a slightly lower value of ∼170 J mol^{-1} K^{-1} has been reported in the related $CH_3NH_3PbCl_3$, $CH_3NH_3PbBr_3$,[16] and $CH_3NH_3SnBr_3$.[29] We suggest that in these hybrid crystals, the heat capacity predicted from classical equipartition of energy is only observed at temperatures well above the Debye temperature of the crystal because of rigid localized modes associated with the molecular ion.

Direct calorimetric evidence of the glass transition in $HC(NH_2)_2PbI_3$ is seen in the feature between 46 K and 51 K. This subtly enhanced heat capacity for the dynamically disordered state above the transition is not detectable in $CH_3NH_3PbI_3$, consistent with its stronger glass dynamics.[25] The apparent small discrepancy in glass transition temperature from the dielectric spectroscopy and from calorimetry is explained by sample temperature equilibration in the dielectric measurements as the sample was swept in the cooling direction for the dielectric data in Figure 2.

Examination of the low temperature heat capacity on a plot of C/T^3 versus T, shown in Figure 5, supports the hypothesis of glassy static disorder in both compositions. The heat capacity of the crystal deviates substantially from the $\sim T^3$ scaling predicted by the Debye model at low temperatures, as indicated by the low temperature "hump" in the C/T^3 versus T plot.[30,31] Systems with glassy disorder are well-known to exhibit heat ca-

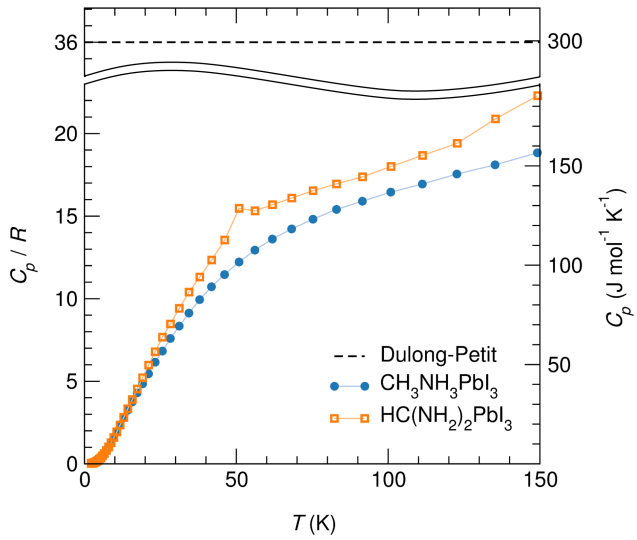

Figure 4: Low and intermediate temperature heat capacity of $CH_3NH_3PbI_3$ and $HC(NH_2)_2PbI_3$, scaled by the gas constant and in absolute units. Error bars are smaller than the markers for all points and are omitted. A glass transition in $HC(NH_2)_2PbI_3$ is evident between 46 K and 51 K while none is detectable in $CH_3NH_3PbI_3$, consistent with stronger glass dynamics in the latter compound.[25]

pacity in excess of that which can be attributed to acoustic phonons, though the exact origin of the corresponding "Boson peak" in the vibrational density of states is still an active area of research.[32–34] The modeled curves in Figure 5 for various Debye temperatures assume a single *A*-site atom rather than a molecule, a simplified model that nonetheless reflects the negligible occupancy of high frequency intramolecular modes at low temperatures. It is not possible to accurately determine Debye temperatures from these data: the heat capacities deviate substantially from the Debye model at low temperatures, and at intermediate temperatures the assumption of linear phonon dispersion is invalid for real crystals, particularly these hybrid systems with molecular ions.

The broader hump in C/T^3 for $HC(NH_2)_2PbI_3$ is consistent with our assertion that this compound exhibits greater glass fragility than $CH_3NH_3PbI_3$.[30] Liu and Löhneysen have compiled the maximum of C/T^3 and the corresponding temperature for a variety of amorphous and crystalline solids, and determined a scaling relation between these two parameters.[35] By comparison with their data, the hybrid perovskites measured here (parameters given in Table 1) fall in the region of polymeric and chalcogenide glasses.[35] Specifically,

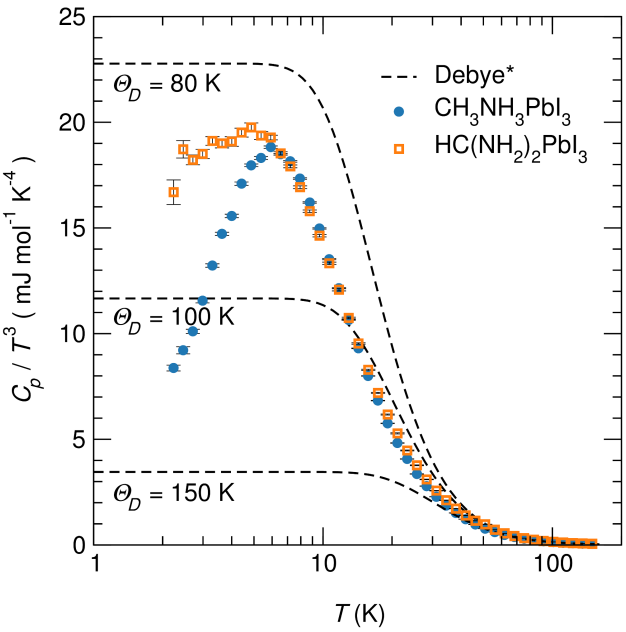

Figure 5: Heat capacity, expressed as C/T^3, of $CH_3NH_3PbI_3$ and $HC(NH_2)_2PbI_3$, illustrating deviation at low temperatures from the expected $C \propto T^3$ acoustic phonon contribution from the Debye model. *The heat capacities calculated from the Debye model assume the *A*-site cation is a single atom rather than a molecule, a simplified model that nonetheless accounts for the negligible activation of the stiffer rotational and vibrational modes of the molecule at low temperatures.

they are most similar by these metrics to poly(methyl methacrylate), polybutadiene, and Apiezon N Grease,[35] offering possible clues about the types of disorder and localized vibrational modes present in their ground state structures.

Table 1: Peak value, $P_c = (C/T^3)_{T=T_{max}}$, of the transformed heat capacity and corresponding temperature, T_{max}, for $CH_3NH_3PbI_3$ and $HC(NH_2)_2PbI_3$.

Sample	T_{max} (K)	P_c (μJ g^{-1} K^{-4})
$CH_3NH_3PbI_3$	5.92	30.4
$HC(NH_2)_2PbI_3$	4.87	31.2

Careful examination of the literature suggests a degree of universality to this glassy behavior in hybrid main group halides and related materials. Similar low temperature dielectric loss dispersion has been reported but has not been adequately explained for $CH_3NH_3PbBr_3$, $CH_3NH_3PbI_3$,[12] and $CH_3NH_3SnBr_3$.[29] In these materials, no glass transition is observed directly in calorimetry[16,29] suggesting an entropic subtlety to the effect and correspondingly strong glass dynamics. Computational studies of $CH_3NH_3SnBr_3$ suggest many nearly degenerate possible ground state structures,[9] which implies a tendency towards glassy configurations. In the hybrid framework $(CH_3)_2NH_2Zn(HCOO)_3$, which adopts the perovskite structure and exhibits similar disorder-driven dielectric transitions to $CH_3NH_3PbI_3$,[36] glassy behavior and an associated memory effect have been observed via temperature-dependent ^{1}H NMR and low temperature calorimetry.[37] A glassy slowing of dynamics similar to those reported in this work is widely observed in "plastic crystals," which are composed of weakly interacting globular molecules that are orientationally or conformationally disordered.[38] We suggest that we may conceptualize the hybrid perovskites as a special case of plastic crystal, with a sublattice of isolated, disordered molecules embedded in an extended (and nominally ordered) inorganic framework. In contrast to conventional glasses that lose translational symmetry, quenched plastic crystals (such as the hybrid perovskites considered here) exhibit static local displacements and orientational disorder but maintain long-range translational periodicity of the molecular units. Recently, the analogy to plastic crystals has been identified and the possibility

of orientationally glassy behavior has been predicted.[39] In the same work, a theoretical framework for treating the dynamically disordered cations and couplings between molecular rotations and lattice vibrations has been proposed.[39]

The precise mechanism behind this glassy disorder in APbI$_3$ is unclear. In $CH_3NH_3PbI_3$, early structural models based on transition entropies imply fully ordered molecular cations in the orthorhombic phase,[16] and ab initio calculations suggest high barriers to cation twisting about the C–N axis if the inorganic framework is rigidly fixed.[18] However, experimental evidence from quasi-elastic and elastic neutron scattering suggests substantial dynamic disorder down to at least 70 K (the lowest temperature probed),[11,17] and it is likely that rotational barriers could be lowered significantly in the presence of distortions of the soft Pb–I network. The same computational study suggests that freezing of a C–N axis twisting motion at an orientation off of a nominal three-fold alignment is energetically unlikely.[18] It is possible that more complex motions are important. A "wobbling-in-a-cone" libration has been identified in $CH_3NH_3PbI_3$ at room temperature ($\sim$300 fs) from 2-D vibrational spectroscopy,[40] and it is possible that similar motions persist in the orthorhombic phase. In light of the attractive interaction between the amine group hydrogens and the iodides of the inorganic cage, it is unlikely that such wobbling would ultimately freeze in an incoherent fashion unless it is accompanied by local distortions of the surrounding Pb–I framework. Low temperature analyses of the crystal structure have not been reported, and it is conceivable that the ground state of this material exhibits complex coupled disorder, perhaps including incommensurate modulation of the organic and inorganic sublattices.[41]

In the absence of low temperature crystal structure models for $HC(NH_2)_2PbI_3$, few mechanistic conclusions can be drawn for this composition. This material presents a prime opportunity for future study: compared to $CH_3NH_3PbI_3$, the effects of the larger molecule with a smaller dipole moment and multiple amine groups will be illuminating. The evidence presented here of low temperature glassy behavior provides new insights towards a complete description of crystal structure and disorder in this curious and promising family

of materials.

Experimental Methods

Single crystals of $CH_3NH_3PbI_3$ and polycrystalline samples of both compositions were prepared via previously reported methods.[10] Due to the slow spontaneous conversion at ambient temperatures of the black perovskite phase of $HC(NH_2)_2PbI_3$ to the yellow phase of 1-D chains of face-sharing PbI_6 octahedra,[10] $HC(NH_2)_2PbI_3$ samples were fully converted to the perovskite phase just prior to measurement by heating in a glass vial with a hot air gun, with the phase purity confirmed by X-ray powder diffraction.

For dielectric measurements, pellets were prepared by grinding polycrystalline samples and cold-pressing to 9 tons in a 13 mm diameter cylindrical die. Indium contacts were applied via low temperature soldering in a parallel plate capacitor geometry. Capacitance–loss measurements were performed using an Andeen-Hagerling AH 2700A Ultra-precision Capacitance Bridge. The sample environment was controlled using a Quantum Design PPMS, over the temperature range of 1.8 K – 300 K. Real and imaginary components of relative permittivity were calculated using a parallel plate capacitor model.

Heat capacity measurements were carried out between 2.2 K and 150 K via relaxation techniques in a Quantum Design PPMS cryostat under high vacuum (9×10^{-6} torr). For $CH_3NH_3PbI_3$, a single crystal ($\sim$1.5 mm, 5.25 mg) was measured. For $HC(NH_2)_2PbI_3$, polycrystalline samples were ground, mixed with powdered iron (50.41% by mass, to enhance thermal conductivity, observed to be extremely low in both compounds as has been reported for $CH_3NH_3PbI_3$[42]), and cold-pressed to 1 ton in a 3 mm $\times$ 9 mm die. The pellet was shattered, and a flat shard (4.48 mg) was measured. The background was subtracted by separately measuring a similarly prepared sample of the metal diluent (4.90 mg) at the same temperatures: the heat capacity of the composite sample was assumed to be a simple linear combination of that of the perovskite and that of the diluent.

Acknowledgement

This work was supported by the U.S. Department of Energy, Office of Science, Basic Energy Sciences under award number DE-SC-0012541. D.H.F. thanks Dr. Geneva Laurita for helpful discussions and Jaye K. Harada for assistance with dielectric measurements. The research involved the use of shared experimental facilities of the Materials Research Laboratory at UCSB supported by the MRSEC Program of the National Science Foundation under Award No. DMR 1121053.

Supporting Information

Complex permittivity of both compositions over the full temperature range (1.8 K to 300 K); differential scanning calorimetry of $HC(NH_2)_2PbI_3$.

References

(1) Kojima, A.; Teshima, K.; Shirai, Y.; Miyasaka, T. Organometal halide perovskites as visible-light sensitizers for photovoltaic cells. *J. Am. Chem. Soc.* **2009**, *131*, 6050–6051.

(2) Jeon, N. J.; Noh, J. H.; Yang, W. S.; Kim, Y. C.; Ryu, S.; Seo, J.; Seok, S. I. Compositional engineering of perovskite materials for high-performance solar cells. *Nature* **2015**, *517*, 476–480.

(3) Du, M.-H.; Singh, D. J. Enhanced Born charge and proximity to ferroelectricity in thallium halides. *Phys. Rev. B* **2010**, *81*, 144114.

(4) Brgoch, J.; Lehner, A. J.; Chabinyc, M. L.; Seshadri, R. Ab initio calculations of band gaps and absolute band positions of polymorphs of $RbPbI_3$ and $CsPbI_3$: Implications for main-group halide perovskite photovoltaics. *J. Phys. Chem. C* **2014**, *18*, 27721–27727.

(5) Labram, J. G.; Fabini, D. H.; Perry, E. E.; Lehner, A. J.; Wang, H.; Glaudell, A. M.; Wu, G.; Evans, H.; Buck, D.; Cotta, R. et al. Temperature-dependent polarization in field-effect transport and photovoltaic measurements of methylammonium lead iodide. *J. Phys. Chem. Lett.* **2015**, *6*, 3565–3571.

(6) Chin, X. Y.; Cortecchia, D.; Yin, J.; Bruno, A.; Soci, C. Lead iodide perovskite light-emitting field-effect transistor. *Nat. Commun.* **2015**, *6*, 7383.

(7) Knop, O.; Wasylishen, R. E.; White, M. A.; Cameron, T. S.; Van Oort, M. J. M. Alkylammonium lead halides. Part 2. $CH_3NH_3PbX_3$ (X = Cl, Br, I) perovskites: cuboctahedral halide cages with isotropic cation reorientation. *Can. J. Chem.* **1990**, *68*, 412–422.

(8) Swainson, I.; Hammond, R.; Soullière, C.; Knop, O.; Massa, W. Phase transitions in the perovskite methylammonium lead bromide, $CH_3ND_3PbBr_3$. *J. Solid State Chem.* **2003**, *176*, 97–104.

(9) Swainson, I.; Chi, L.; Her, J.-H.; Cranswick, L.; Stephens, P.; Winkler, B.; Wilson, D. J.; Milman, V. Orientational ordering, tilting and lone-pair activity in the perovskite methylammonium tin bromide, $CH_3NH_3SnBr_3$. *Acta Crystallogr. Sect. B Struct. Sci.* **2010**, *66*, 422–429.

(10) Stoumpos, C. C.; Malliakas, C. D.; Kanatzidis, M. G. Semiconducting tin and lead iodide perovskites with organic cations: phase transitions, high mobilities, and near-infrared photoluminescent properties. *Inorg. Chem.* **2013**, *52*, 9019–9038.

(11) Weller, M. T.; Weber, O. J.; Henry, P. F.; Di Pumpo, A. M.; Hansen, T. C. Complete structure and cation orientation in the perovskite photovoltaic methylammonium lead iodide between 100 and 352 K. *Chem. Commun.* **2015**, *51*, 4180–4183.

(12) Onoda-Yamamuro, N.; Matsuo, T.; Suga, H. Dielectric study of $CH_3NH_3PbX_3$ (X = Cl, Br, I). *J. Phys. Chem. Solids* **1992**, *53*, 935–939.

(13) Maeda, M.; Hattori, M.; Hotta, A.; Suzuki, I. Dielectric studies on $CH_3NH_3PbX_3$ (X = Cl and Br) single crystals. *J. Phys. Soc. Japan* **1997**, *66*, 1508.

(14) Wasylishen, R.; Knop, O.; Macdonald, J. Cation rotation in methylammonium lead halides. *Solid State Commun.* **1985**, *56*, 581–582.

(15) Xu, Q.; Eguchi, T.; Nakayama, H.; Nakamura, N.; Kishita, M. Molecular motions and phase transitions in solid $CH_3NH_3PbX_3$ (X = Cl, Br, I) as studied by NMR and NQR. *Zeitschrift für Naturforsch. A* **1991**, *46*, 1–30.

(16) Onoda-Yamamuro, N.; Matsuo, T.; Suga, H. Calorimetric and IR spectroscopic studies

of phase transitions in methylammonium trihalogenoplumbates (II). *J. Phys. Chem. Solids* **1990**, *51*, 1383–1395.

(17) Chen, T.; Foley, B. J.; Ipek, B.; Tyagi, M.; Copley, J. R. D.; Brown, C. M.; Choi, J. J.; Lee, S.-H. Rotational dynamics of organic cations in the $CH_3NH_3PbI_3$ perovskite. *Phys. Chem. Chem. Phys.* **2015**, *17*, 31278–31286.

(18) Lee, J.-H.; Bristowe, N. C.; Bristowe, P. D.; Cheetham, A. K. Role of hydrogen-bonding and its interplay with octahedral tilting in $CH_3NH_3PbI_3$. *Chem. Commun.* **2015**, *51*, 6434–6437.

(19) Weller, M. T.; Weber, O. J.; Frost, J. M.; Walsh, A. Cubic perovskite structure of black formamidinium lead iodide, α-$[HC(NH_2)_2]PbI_3$, at 298 K. *J. Phys. Chem. Lett.* **2015**, *6*, 3209–3212.

(20) Eames, C.; Frost, J. M.; Barnes, P. R. F.; O'Regan, B. C.; Walsh, A.; Islam, M. S. Ionic transport in hybrid lead iodide perovskite solar cells. *Nat. Commun.* **2015**, *6*, 7497.

(21) Sillars, R. The properties of a dielectric containing semiconducting particles of various shapes. *J. Inst. Electr. Eng.* **1937**, *80*, 378–394.

(22) Billig, E.; Plessner, K. W. A note on the dielectric dispersion in polycrystalline materials. *Proc. Phys. Soc. Sect. B* **1951**, *64*, 362–363.

(23) Koops, C. G. On the dispersion of resistivity and dielectric constant of some semiconductors at audiofrequencies. *Phys. Rev.* **1951**, *83*, 121–124.

(24) Dixon, P.; Wu, L.; Nagel, S.; Williams, B.; Carini, J. Scaling in the relaxation of supercooled liquids. *Phys. Rev. Lett.* **1990**, *65*, 1108–1111.

(25) Angell, C. A. Formation of glasses from liquids and biopolymers. *Science* **1995**, *267*, 1924–1935.

(26) Lunkenheimer, P.; Loidl, A. Dielectric spectroscopy of glass-forming materials: α-relaxation and excess wing. *Chem. Phys.* **2002**, *284*, 205–219.

(27) Schneider, U.; Lunkenheimer, P.; Brand, R.; Loidl, A. Broadband dielectric spectroscopy on glass-forming propylene carbonate. *Phys. Rev. E* **1999**, *59*, 6924–6936.

(28) Kittel, C.; Kroemer, H. *Thermal physics*, 2nd ed.; W. H. Freeman and Company: San Francisco, 1980.

(29) Onoda-Yamamuro, N.; Matsuo, T.; Suga, H. Thermal, electric, and dielectric properties of $CH_3NH_3SnBr_3$ at low temperatures. *J. Chem. Thermodyn.* **1991**, *23*, 987–999.

(30) Sokolov, A.; Calemczuk, R.; Salce, B.; Kisliuk, A.; Quitmann, D.; Duval, E. Low-temperature anomalies in strong and fragile glass formers. *Phys. Rev. Lett.* **1997**, *78*, 2405–2408.

(31) Melot, B. C.; Tackett, R.; O'Brien, J.; Hector, A. L.; Lawes, G.; Seshadri, R.; Ramirez, A. P. Large low-temperature specific heat in pyrochlore $Bi_2Ti_2O_7$. *Phys. Rev. B* **2009**, *79*, 224111.

(32) Lubchenko, V.; Wolynes, P. G. The origin of the boson peak and thermal conductivity plateau in low-temperature glasses. *Proc. Natl. Acad. Sci. U. S. A.* **2003**, *100*, 1515–1518.

(33) Safarik, D.; Schwarz, R.; Hundley, M. Similarities in the C_p/T^3 peaks in amorphous and crystalline metals. *Phys. Rev. Lett.* **2006**, *96*, 195902.

(34) Chumakov, A. I.; Monaco, G.; Monaco, A.; Crichton, W. A.; Bosak, A.; Rüffer, R.; Meyer, A.; Kargl, F.; Comez, L.; Fioretto, D. et al. Equivalence of the boson peak in glasses to the transverse acoustic van Hove singularity in crystals. *Phys. Rev. Lett.* **2011**, *106*, 225501.

(35) Liu, X.; Löhneysen, H. V. Specific-heat anomaly of amorphous solids at intermediate temperatures (1 to 30 K). *Europhys. Lett.* **1996**, *33*, 617–622.

(36) Jain, P.; Dalal, N. S.; Toby, B. H.; Kroto, H. W.; Cheetham, A. K. Order–disorder antiferroelectric phase transition in a hybrid inorganic–organic framework with the perovskite architecture. *J. Am. Chem. Soc.* **2008**, *130*, 10450–10451.

(37) Besara, T.; Jain, P.; Dalal, N. S.; Kuhns, P. L.; Reyes, A. P.; Kroto, H. W.; Cheetham, A. K. Mechanism of the order–disorder phase transition, and glassy behavior in the metal-organic framework $[(CH_3)_2NH_2]Zn(HCOO)_3$. *Proc. Natl. Acad. Sci. U. S. A.* **2011**, *108*, 6828–6832.

(38) Sherwood, J. N., Ed. *The plastically crystalline state: orientationally disordered crystals*; John Wiley & Sons: Chichester, 1979.

(39) Even, J.; Carignano, M.; Katan, C. Molecular disorder and translation/rotation coupling in the plastic crystal phase of hybrid perovskites. *Nanoscale* **2016**, *in press.*

(40) Bakulin, A. A.; Selig, O.; Bakker, H. J.; Rezus, Y. L.; Müller, C.; Glaser, T.; Lovrincic, R.; Sun, Z.; Chen, Z.; Walsh, A. et al. Real-time observation of organic cation reorientation in methylammonium lead iodide perovskites. *J. Phys. Chem. Lett.* **2015**, *6*, 3663–3669.

(41) Swainson, I. P. Tilt and acoustic instabilities in ABX_4, A_2BX_4 and ABX_3 perovskite structure types: Their role in the incommensurate phases of the organic–inorganic perovskites. *Acta Crystallogr. Sect. B Struct. Sci.* **2005**, *61*, 616–626.

(42) Pisoni, A.; Jaćimović, J.; Barišić, O. S.; Spina, M.; Gaál, R.; Forró, L.; Horváth, E. Ultra-low thermal conductivity in organic–inorganic hybrid perovskite $CH_3NH_3PbI_3$. *J. Phys. Chem. Lett.* **2014**, *5*, 2488–2492.

>>> Supporting Information <<<

Dielectric and Thermodynamic Signatures of Low Temperature Glassy Dynamics in the Hybrid Perovskites $CH_3NH_3PbI_3$ and $HC(NH_2)_2PbI_3$

Douglas H. Fabini,[†,‡] Tom Hogan,[¶,‡] Hayden A. Evans,[†,§] Constantinos C. Stoumpos,[‖] Mercouri G. Kanatzidis,[‖] and Ram Seshadri[*,†,‡,§]

†*Materials Research Laboratory, University of California, Santa Barbara, California 93106, USA*

‡*Materials Department, University of California, Santa Barbara, California 93106, USA*

¶*Department of Physics, Boston College, Chestnut Hill, Massachusetts 02467, USA*

§*Department of Chemistry and Biochemistry, University of California, Santa Barbara, California 93106, USA*

‖*Department of Chemistry and Argonne-Northwestern Solar Energy Research (ANSER) Center, Northwestern University, Evanston, Illinois 60208, USA*

E-mail: seshadri@mrl.ucsb.edu

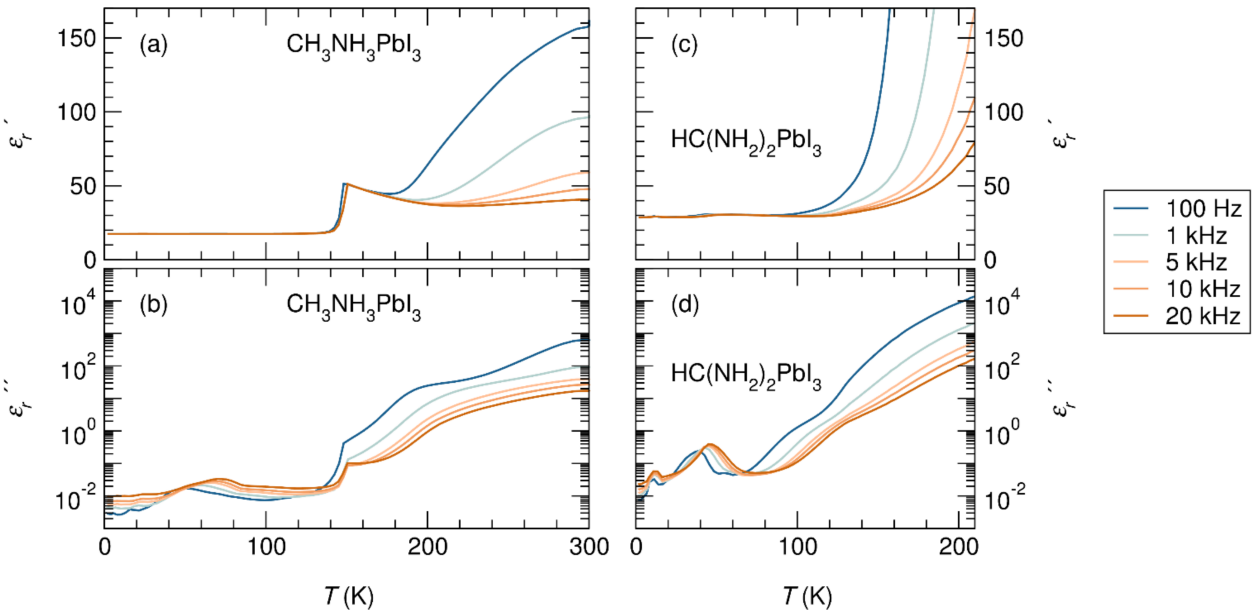

Figure S1: Real (ϵ_r') and imaginary (ϵ_r'') parts of the relative permittivity of polycrystalline (a,b) $CH_3NH_3PbI_3$ and (c,d) $HC(NH_2)_2PbI_3$ extracted from capacitance–loss measurements. The tetragonal-to-orthorhombic phase transition in $CH_3NH_3PbI_3$ at 160 K is accompanied by a steep drop in ϵ_r', consistent with the loss of tumbling degrees of freedom of the $CH_3NH_3^+$ cation. In the high temperature regime, the intrinsic permittivity is obscured by possible ionic conductivity[1–4] as well as interfacial and microstructural effects[5–7] that manifest as greatly enhanced apparent permittivity and loss.

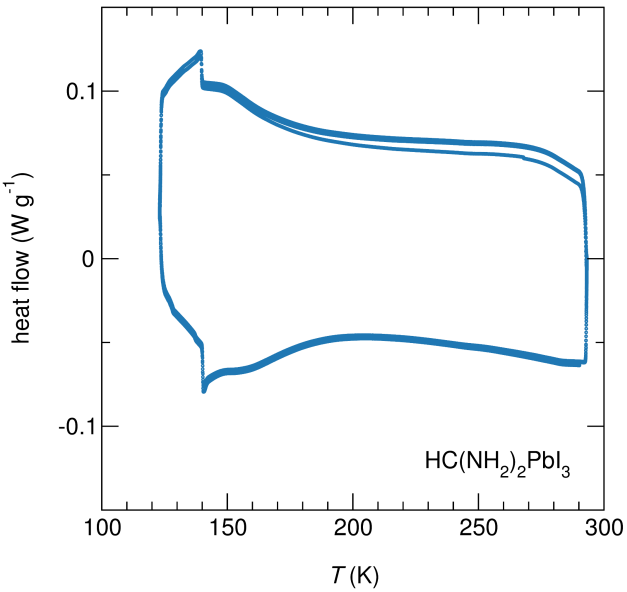

Figure S2: Differential scanning calorimetry of the phases of $HC(NH_2)_2PbI_3$ corresponding to the black, 3-D connected perovskite structure at ambient temperature. A first-order phase transition is evident at 140 K.

References

(1) Labram, J. G.; Fabini, D. H.; Perry, E. E.; Lehner, A. J.; Wang, H.; Glaudell, A. M.; Wu, G.; Evans, H.; Buck, D.; Cotta, R. et al. Temperature-dependent polarization in field-effect transport and photovoltaic measurements of methylammonium lead iodide. *J. Phys. Chem. Lett.* **2015**, *6*, 3565–3571.

(2) Chin, X. Y.; Cortecchia, D.; Yin, J.; Bruno, A.; Soci, C. Lead iodide perovskite light-emitting field-effect transistor. *Nat. Commun.* **2015**, *6*, 7383.

(3) Eames, C.; Frost, J. M.; Barnes, P. R. F.; O'Regan, B. C.; Walsh, A.; Islam, M. S. Ionic transport in hybrid lead iodide perovskite solar cells. *Nat. Commun.* **2015**, *6*, 7497.

(4) Maeda, M.; Hattori, M.; Hotta, A.; Suzuki, I. Dielectric studies on $CH_3NH_3PbX_3$ (X =Cl and Br) single crystals. *J. Phys. Soc. Japan* **1997**, *66*, 1508.

(5) Sillars, R. The properties of a dielectric containing semiconducting particles of various shapes. *J. Inst. Electr. Eng.* **1937**, *80*, 378–394.

(6) Billig, E.; Plessner, K. W. A note on the dielectric dispersion in polycrystalline materials. *Proc. Phys. Soc. Sect. B* **1951**, *64*, 362–363.

(7) Koops, C. G. On the dispersion of resistivity and dielectric constant of some semiconductors at audiofrequencies. *Phys. Rev.* **1951**, *83*, 121–124.